Thermally stable, conductive and flame-retardant nylon 612 composites created by adding two-dimensional alumina platelets

Pingan Song, Cong Wang, Lei Chen, Yiqi Zheng, Lina Liu, Qiang Wu, Guobo Huang, Youming Yu, Hao Wang

PII: S1359-835X(17)30095-7
DOI: http://dx.doi.org/10.1016/j.compositesa.2017.02.029
Reference: JCOMA 4590

To appear in: *Composites: Part A*

Received Date: 22 November 2016
Revised Date: 18 January 2017
Accepted Date: 28 February 2017

Please cite this article as: Song, P., Wang, C., Chen, L., Zheng, Y., Liu, L., Wu, Q., Huang, G., Yu, Y., Wang, H., Thermally stable, conductive and flame-retardant nylon 612 composites created by adding two-dimensional alumina platelets, *Composites: Part A* (2017), doi: http://dx.doi.org/10.1016/j.compositesa.2017.02.029

Thermally stable, conductive and flame-retardant nylon 612 composites created by adding two-dimensional alumina platelets

Pingan Song[1,2,#,*], Cong Wang[2,#], Lei Chen[2,#], Yiqi Zheng[2,#], Lina Liu[2], Qiang Wu[2], Guobo Huang[3], Youming Yu[2], Hao Wang[1,*]

[1] *Centre for Future Materials, University of Southern Queensland, Toowoomba, 4350, Australia*

[2] *Department of Materials, Zhejiang A&F University, Hangzhou, 311300, China*

[3] *School of Pharmaceutical and Chemical Engineering, Taizhou University, Taizhou, 31700, China*

Corresponding Authors

*E-mail: Pingan.Song@usq.edu.au, Hao.Wang@usq.edu.au

ABSTRACT: With growingly demands for better performances in electronic-related applications, further improving thermal and fire safety of nylon 612 (PA612) becomes extremely pressing. In this work, we have reported the fabrication of flame retardant and thermally stable and conductive PA612 composites by using two-dimensional alumina platelets. Alumina platelets are observed being uniformly dispersed within the PA612 matrix. Thermal analysis demonstrates that addition of alumina platelets noticeably increases thermal stability and conductivity of PA612. Cone calorimetry results show that 40 wt% of alumina platelets addition decreases the peak heat release rate (pHRR) and total smoke production of PA612 by 54% and 29%, respectively, indicating largely enhanced flame resistance. Rheology tests demonstrate that there exists a nearly qualitative correlation between the flammability (pHRR) and viscoelastic behaviours (storage modulus). This work offers a new approach for creating advanced polymer composites with enhanced thermal and flame retardancy properties by using alumina platelets as multifunctional filler.

Keywords: A. Polymer-matrix composites (PMCs); A. Plates; B. thermal property; B. Rheological properties

1. Introduction

Polyamides (PAs), such as PA46, PA6, PA66, PA11 and PA612 are one category of commercially significant engineering plastic materials with growingly extensive application. Among PAs, PA612 (nylon 612) possesses balanced mechanical properties, excellent abrasion and chemical resistance and ease of processing due to its intermediate carbon chain [1-5]. Moreover, PA612 features better ductility and dimension stability as well as lower moisture sensitivity as compared with typical PA6 and PA66 4-5]. These features enable PA612 to find increasingly wide applications covering precision mechanical components, automobile manufacturing, electric and electronic appliances, and aerospace engineering [4-6].

Similar to PA6, in spite of featuring self-extinguishment, PA612 still fails to meet the flame resistance requirements when used in the electric and electronic fields, such as electric wires, cables, and devices [7-8]. In addition, upon combustion it generates large amount heat accompanied by melt dripping and a large amount of smoke, thus posing a huge potential fire threat to human lives and their belongings. Generally, adding flame retardants (FRs) is one facile and effective approach to improve the flame retardancy of polymeric materials. Until now a variety of FRs have been adopted to enhance the fire safety of PAs, but mainly on PA6 and PA66 [7-8]. Currently, the typical FRs include nitrogen- [7,9], phosphorus- [10,11], phosphorus-nitrogen-based compounds [12-14], and inorganic magnesium hydroxide,[8,15] as well as the recently emerged nanoscale materials , such as one-dimensional (1D) carbon nanotubes [16] and titanate nanotubes [17], and two-dimensional (2D) clay [18], MoS_2 [19,20] and graphene [21-23].

Alumina (Al_2O_3) nanoparticles, especially after surface modification, have recently shown to be capable of remarkably increasing the thermal stability and flame

resistance of polystyrene (PS) and poly (methyl methacrylate) (PMMA), despite some alumina agglomerates being observed in the polymer matrix [24,25]. For this reason, we assume that 2D alumina platelets are expected to theoretically enhance the thermal and flame resistance properties of PA612 by acting as a thermal insulation layer like other 2D materials, such as graphene, MoS_2 and clay [18-23] during burning. In addition, 2D alumina platelets with lower aspect ratio are much easier to disperse in the polymer matrix as compared with other nano-sized alumina counterparts with much higher aspect ratio.

Hence, the objective of this work is to examine effects of 2D alumina platelets on the thermal stability and flammability properties of PA612. To enhance the interfacial adhesions with PA612, alumina platelets were amino-functionalized prior to melt blending. Results show that thermal stability and conductivity of PA612 can increase considerably with the addition of alumina platelets. Besides, 2D alumina platelets are capable of remarkably reducing the peak heat release rate and total smoke production of PA612 because of the formation of the thermal insulation char layer during combustion. This work provides a novel approach for creating highly thermally stable, conductive and flame-retardant polymer composites by using 2D inorganic fillers as building blocks.

2. Experimental

2.1. Material and methods

PA612 resin (Zytel 158L, density: 1.06 g/cm^3) was obtained from DuPont China Holding., Co., Ltd. Alumina platelets (density: ~3.97 g/cm^3) were purchased from Antaria Co., Ltd, Australia. N-(2-aminoethyl)-3-aminopropyltrimethoxysilane (N2E3APTMS) was bought from Zhejiang Feidian Chemical Co., Ltd (China). The

processing aids (antioxidant 1010/168) were purchased from Jinan Aimin Chemical Co., Ltd. (Shandong, China). Other chemicals, such as ethanol, were analytical grade and directly used without further purification.

2.2. Surface modification of Al_2O_3 platelets

According to the modification approach reported [26,27], typically, 10 mL of N2E3APTMS was added into a 250 mL flask with 90 mL of methanol and 10 mL of deionized water, and the mixture was stirred for half an hour to fully hydrolyze the silane coupling agent. Then, 50 g of Al_2O_3 platelets were added into the solution and sonicated for 15 min, followed by stirring the mixture at 60 ^oC for 3 hours. Finally, the mixture was filtered and dried at 80 ^oC until the weight remained constant. About 50.28 g modified Al_2O_3 (designated as NH_2-Al_2O_3) was obtained, which means that the as-prepared NH_2-Al_2O_3 contains 0.56 wt% of silane surface modifier.

2.3. Composite fabrication

PA612 composites were prepared according to the preset formulation via melt compounding the surface modified alumina with PA612 resin using a ThermoHaaker Torque Rheometer (Germany). The loading level of antioxidants was set at 0.5 wt% of the total weight of each sample. All composites were melt-compounded at 215 ^oC for 10 min with a rotor speed of 60 rpm. Subsequently, all samples were hot-pressed at 8 MPa into samples with standard size for further measurements. As for the designation, for example, the composite containing 20 wt% alumina platelets was named PA/20% AP, and the PA612 matrix was designated as the PA612 bulk. The PA612 matrix was also prepared using the same procedure for comparison.

2.4. Characterization

Field emission scanning electron microscope (FEI-SEM, S4800) was used to observe the morphology of alumina platelets and the dispersion in the polymer matrix at an accelerating voltage of 5 kV. The morphology of alumina was also obtained on a transmission electron microscopy (TEM, JEOL JEM-1230). Differential scanning calorimeter (DSC Q600) was used to determine the glass transition temperature (T_g) and melt behaviors of PA612 composites with a heating rate of 10 ^oC/min in a temperature range of 25 to 230 ^oC. Each specimen was first heated from 25 to 240 ^oC to remove the residual thermal history and then held at 230 ^oC for 3 min prior to cooling down to -60 ^oC at a cooling rate of 10 ^oC/min followed by further heating (second heating cycle) at a heating rate of 10 ^oC/min to 230 ^oC. The degree of crystallinity, χ_c (%) is calculated by using following Eq. (1):

$$\chi_c(\%) = \frac{\Delta H_m \bullet w}{\Delta H_{m0}} \times 100 \qquad (1)$$

where, ΔH_m refers to the heat of fusion of PA612, the heat of fusion of 100% crystalline PA-612 ΔH_{m0} is taken as 258 J/g [5]and w is the mass fraction of matrix PA612 in the blends.

Thermogravimetric analysis (TGA) tests were carried out on a TASDTQ600 (TA Instruments, USA) thermogravimetric analyzer. Typically, about 8.0 mg of sample was heated from room temperature to 700 ^oC at a heating rate of 20 ^oC /min under both nitrogen and air atmosphere. Thermal conductivity was performed on a DRL-III Thermal conductivity tester (Shanghai Jiezhun Instrument Co., Ltd, China). The flammability properties of samples were evaluated using a cone calorimeter in an FTT UK device according to ISO 5660 with an incident flux of 35 kW/m^2. The sample has a size of 100 ×100 ×3.0 mm^3. Typically the results from the cone calorimeter tests can be reproduced within 5 % and the data reported here were the means of triplicate

experiments. The limited oxygen index (LOI) was measured on a JF-3 oxygen index meter (Jiangning, China) with sheet dimensions of 130 ×6.5 × 3 mm^3 according to ISO4589-1984. The UL-94 rating was tested according to the UL-94 (ASTM D 63577) standard. Rheological measurements were performed on an ARES-G2 (TA Instrument, USA) in a dynamic mode on parallel-plate geometry with a diameter of 25 mm and a gap of around 1 mm. The testing temperature was 220 ^{o}C with a frequency range of 0.01585-100 rad/s at a strain of 10 % to make it within the linear viscoelastic range.

3. Results and discussions

3.1. Morphology

Fig. 1 shows typical morphologies of the original 2D alumina platelets used in this work. Evidently, alumina platelets exhibit an thickness range from 200 to 500 nm (Fig. 1A) and an average diameter of 7.5 μm (Fig.1B), which means a relatively low aspect ratio of ~35. Figure 1 also displays its dispersion in the PA612 matrix after surface modification. At a relatively low loading level, such as 5 wt% (Fig. 1C) and 10 wt% (Fig. 1D), some alumina platelets are clearly visible and well-dispersed on the fracture surface, as marked by blue arrows. Even with regard to the PA/20%AP sample (Fig. 1E), alumina can also be homogeneously dispersed in the matrix resin without much of agglomeration. Such good dispersion are mainly attributed to two aspects: one is the relative low aspect ratio of alumina, and the other is that after modification alumina platelets can form strong interfaces with the PA612 matrix via hydrogen bonding interactions between amino groups (-NH_2) on the alumina platelets surfaces and the aminocarbonyl groups in PA612 chains.. On the other hand, strong interfacial hydrogen-bond interactions also enable neighbouring alumina platelets to readily stack together to form micro-agglomerates especially at a very high loading level. For

instance, a few alumina platelets are observed to stack together in the PA/40 %AP sample, marked by the red circle (see Fig. 1F).

3.2. Glass transition and crystallization

The presence of alumina platelets are expected to unavoidably affect the thermal properties, especially the glass transition tempreature (T_g) and melt behaviors of PA612. As shown in Fig. 2 and Table 1, the PA612 matrix displays a T_g of 56.8 ^oC and bascially the T_g value rises monotonously with increasing loading level of alumina platelets. For instance, addition of 10 wt% and 40 wt% of alumina enables T_g to increase by 1.8 ^oC and 3.4 ^oC, respectively. This strongly indicates that the presence of alumina platelets is capable of considerably restricting the movement of PA612 chains by the steric hindrance effect of alumina platelets and the interfacial interactions between them, thus leading to a higher T_g. Similar increase in T_g was also oserved in titnnate nanotubes filled PA11 system [17]. Such increased T_g values are very critical to increase the upper limit of the service termperature for PA612, which can extend its engineering applications.

It seems that the addition of alumina platelets has a neglected impact on the melt behavior of PA612, and all composites display a close main melting point (T_{m1}) at around 215.6^oC. Interestingly, a small shoulder melt peak (T_{m2}) at 200.3 ^oC also appears in the DSC thermograms for the pristine PA612 and all composites. However, it is not obvious in the first heating cycle, indicating that it is likely attributed to the secondary crystallization of PA612 chains in the process of cooling, and both melt peaks should arise from the α-phase crystal of PA612 [28,29]. Unexpectedly, when the loading level of alumina increases up to 40 wt%, another melt peak (T_{m3}) appears at a very low temperature of only 129.6 ^oC, about 86 ^oC lower than that of the main melt peak. This endothermic peak was reported to belong to the melting of the γ-

phase crystalline region relating to the reflection of crystalline plane (100) of PA612 [27, 29,30]. This indicates that the a great quantity of alumina platelets can induce the formation of γ-phase crystalline, as evidenced by X-ray diffraction results [27,29].

As for the degree of crystallinity (χ_c), similar to the main melting point, it basically remains unchanged when loaded with alumina platelets except for PA/40% AP (see Table 1), clearly suggesting that the presence of alumina platelets has a limited impact on the crystallinity of PA612 in spite of strong interfacial interactions between them. However, 40 wt% of alumina platelets makes χ_c sharply drop from 18.4% for the PA612 bulk to 13.5 %. This is partially because the presence of a large quantity of alumina platelets dramatically restricts the rearrangement of the PA612 chain segment. Meanwhile, the hydrogen-bond interactions between alumina platelets and PA612 chains replace some of those originally exist among the latter, inevitably reducing to some extent the driving force of crystallization in the cooling process. These two aspects bring about a low degree of crystallinity.

3.3. Thermal stability

Evaluation of the thermal stability of PA612 can contribute to understanding the combustion behavior since small moleclular degradation products generated can act as fuel to accelarate the combustion. It is evident to observe from Fig. 3 that in N_2 condition the pure modified alumina is very thermally stable with only 0.34 wt% mass loss observed up to 700 ^{o}C, which probably due to the degradation of silane modifier. In comparison, the PA612 exihibits a typical one-step decomposition, starts at about 428 ^{o}C (T_i, the temperature where 5 wt% mass loss occurs) and decomposes the most rapidly at around 473 ^{o}C (T_{max}, the temperature where the maximum weight loss takes place), indicating a relatively high thermal stability in an inert atmobphere. Upon loaded with alumina platelets, both T_i and T_{max} values of composites increase steadily

with increasing loading level of alumina. For instance, T_i increases by 7 ^oC for PA/10% AP and 19 ^oC for PA/40% AP (447 ^oC) while T_{max} rises from 473 ^oC to 480 ^oC for PA/10% AP and then to 487 ^oC for PA/40% AP. This means that the presence of alumina platlets is capable of remarkably enhancing thermal stability of PA612, especially the T_i, mainly due to the presence of thermally stable 2D alumina in PA612. By contrast, adding alumina nanoparticels only leads to the slight reduction in both T_i and T_{max} values in N_2 condition because they are less effective in forming thermal insulation barrer for protecting PMMA [25] because of its spherical morphology. With respect to structurally analogous nanoclay, instead of increase, 5.0 wt% of nanoclay slightly reduces the thermal stability of PA6 probably due to the thermal degradation of the organic modifier [18].

In terms of the char residue, for pure PA612 there is hardly any residue char left after 700 ^oC in nitrogen condition, whereas for the PA612 composites the residue char is found to increase monotonously with increasing alumina loading levels. For PA/20%AP and PA/40%AP, the char residue is around 20 wt% and 37.6 wt% respectively, basically corresponding to the alumina content. It is understandable that the char residue can act as a physical barrier to create a tortuous path for the transfer of small molecular degradation products from the heated polymer bulk, thus making PA612 show enhanced thermal stability (for instance, T_{max}).

TGA in air condition allows us to further understand the thermal oxidative stability of PA612 because the participation of oxygen can catalyze the thermal decomposition and most polymeric materials are normally used in air. As shown in Fig. 4, on the whole TGA results in air show a similar trend to those in N_2. Both thermal stability parameters, T_i and T_{max}, of PA612 composites gradually increase with increasing alumina content but the magnitude of increase in the two parameters are much higher

than those in nitrogen condition. For instance, the PA612 bulk displays a T_i of 404 ^oC and a T_{max} of 466 ^oC in air, both of which are far lower than the corresponding value in nirtogen because of the oxidation action induced by oxygen. However, adding 10% of alumina enables T_i and T_{max} to respectively increase up to 421 ^oC and 470 ^oC, and for 40% of alumina filled PA612 T_i and T_{max} are enhanced by 32 ^oC and 21 ^oC respectively as compared with the pristine PA612. By contrast, alumina nanoparticles were also reported to remarkably increase the thermal oxidative stability of PMMA and polystyrene (PS) via absorbing polymer chains onto the nanoparticle surface [24] and changing the decomposition mechanism. However, it is interesting to compare that incorporating one-dimensional multiwall carbon nanotubes (MWNT) hardly leads to improved thermal stability of PA6 even if the formation of network-like structure in the polymer matrix [16]. In case of our system, 2D alumina platelets are likely to be able to create a network-like physical barrier, which can reduce dramatically the diffustion of oxygen from the sample surface to the polymer bulk, thus resulting in a largely enhanced thermal oxidative stability. In other words, it is primarily the thermal protection action of 2D alumina paltelets that governs the remarkably enhanced thermal stability of PA612 regardless of the testing atmospheres.

To better understand effects of 2D alumina on the thermal stability proerties of PA612, we attempt to unlock the relationship between the enhancement of thermal stability and the loading levels of alumina platelets. As expected, it is clear from Fig. 5 that there exists a linear relationship between T_i (or T_{max}) and the volume fraction ($\square_a$) of alumina platelets except some deviation for T_i in air condition. T_i and T_{max} of PA612 composites can be expressed as the following equations (2-5):

$$T_i(^oC) = 429 + (122 \pm 4)\phi_a \quad (\text{in } N_2) \qquad (2)$$

$$T_{max}(^oC) = 475 + (76 \pm 2)\phi_a \quad (\text{in } N_2) \qquad (3)$$

$$T_i(^oC) = 404 + (211 \pm 5)\phi_a \quad \text{(in air)} \qquad (4)$$

$$T_{max}(^oC) = 467 + (122 \pm 3)\phi_a \quad \text{(in air)} \qquad (5)$$

where, the intercept in above four equations basically corresponds with the T_i or T_{max} value of the PA612 matrix, whereas the slope (k) can reflect the degree of impact of alumina content on the property improvement of PA612. Evidently, the k value in air are much higher that in N_2 for the corresponding parameter, e.g. 211 (in air) higher than 122 (in N_2) for T_i, while 122 (in air) versus 76 (in N_2) for T_{max}. This further indicates that alumina platelets have a much higher positive effect on improvements of thermal stability of PA612 in air than in nitrogen atmosphere through the thermal barrier action. These simple relationships are also found in our previous poly(vinyl alcohol) system cross-linked by mutliple hydrogen bonds [31,32], which can offer guidelines to design thermally stable polymeric composites.

3.4. Thermal conductivity

On the other hand, it is well-known that alumina has been widely used as thermally conductive fillers for many materials [33, 34]. Therefore, the addition of alumina platelets is assumed to result in a higher thermal conductivity, which has an adverse affect on the thermal stability of PA612. That is to say, the high thermal conductivity of alumina may affect the thermal barrier effect on the polymer. Unexpectedly, it is found that the thermal conductivity hardly has a negative effect on the thermal stability (T_i and T_{max}), and instead there nearly exists a positive correlation between them at relatively low content of alumina (see Figs.3-6). In other words, they basically share a similar change trend with increasing loading levels of alumina to some extent. As presented in Fig. 6, as compared with the PA612 matirx the thermal conductivity (λ) is also observed to steadily rise with increasing loading levels of alumina up to 20 wt%. For instance, adding 10 wt% and 20 wt% of alumina enables the λ (0.32 W/mK

for PA612) to increase by 19 % (0.38 W/mK) and by 44 % (0.46 W/mK), respectively. Such improvements can be ascribed to the high thermal conductivity of alumina platelets (~ 30 W/mK) [33,34] and the uniform deispersion in the polymer matrix. However, upon increasing the loading level of alumina above 20 wt%, the conductivity slightly drops (30 wt% of alumina) followed by rebounding when the loading level reaches up to 40 wt%. This is probably because some alumina platelets tend to stack together to form agglomerates because of strong interactions among platelets once the loading level is above 30 wt%, thus instead leading to the reduction of the effective loading level. In case of PA612 filled with 40 wt% alumina, the increase of alumina content can make up the loss of loading levels due to alumina stacking, as observed in the Fig. 1E&F.

In addition, we employ the several models to validate experimental results. The thermal conductivity of composites, λ_c, can be expressed by the following Eqs. 6-8 [35,36].

$$\lambda_{c\parallel} = \lambda_p(1-\phi_a) + \lambda_a\phi_a \qquad (6)$$

$$\lambda_{c\perp} = 1/[(1-\phi_a)/\lambda_p + \phi_a/\lambda_a] \qquad (7)$$

$$\lambda_c = \lambda_p^{(1-\phi_a)} + \lambda_a^{\phi_a} \qquad (8)$$

where $\lambda_{c\parallel}$ and $\lambda_{c\perp}$ are repectively the largest two-phase system thermal conductivity (the system represents as a parallel set of plates (phases) extending in the direaction of heat flow and the smallest thermal conductivity (the plates (phases) are stacked in series with respect to the direction of heat flow. □ is the volume fraction of alumina, and subscripts, c, a and p refer to the composite, alumina and polymer, respectively.

Obviously, the experimental λ values of all composites fall between the $\lambda_{c\parallel}$ and $\lambda_{c\perp}$. It seems that the exponential relatioship (Eq. 8) is able to better predict the change trend of λ of composites due to the uniform dispersion of alumina with a ϕ_a < 10.3 vol%

(30 wt%). Despite that, the predicted values are slightly smaller than the experimental ones, which is most likely due to the relatively higher aspect ratio of 2D alumina than spherical counterparts. The deviation turn much more obvious because of the alumina aggregation upon $\square_a$>10.3 vol%.

3.5. Flame resistancy

Cone calorimetry is one extremely powerful tool for evaluating the flammability of a material as it can simulate the real combustion behavior in fire on a small scale, providing us much critical and reliable fire information [37,39]. Among all the information collected from cone tests, heat release and smoke production are two crucial parameters. A large amount of heat release can cause the trapped people to get burned whereas thick smoke leads to low visibility, thus reducing the chance of people in fire to escape from fire hazards.

As shown in Fig. 7A and Table 2, the PA612 matrix display a time to ignition (t_{ign}) of 46 s, peak heat release rate (pHRR) of 875 kW/m^2 and total heat release (THR) of 27.9 MJ/m^2, indicating that PA612 is relatively flammable and releases a great deal of heat upon burning. In addition, it burns very rapidly with 16 wt% of char residue left after the cone test. In comparison, the presence of alumina platelets only has a marginally negative impact on the t_{ign} of PA612, namely leading to a reduction in t_{ign} to a limited degree. Unexpectedly, the PA/30% AP sample displays the longest t_{ign} of 57s, even 11s longer than that of the PA612 matrix, which seems to correlate with a relatively low thermal conductivity as compared with that of PA/20% AP or PA/40% AP (see Fig. 6). With respect to the heat release, both pHRR and THR basically drop monotonously upon adding alumina and with increasing the loading level (see Fig. 7 and Table 2). 20 wt% of alumina platelets enables the pHRR and THR of PA612 to reduce by 47% and 14%, whereas 40 wt % of alumina leads to a noticeable reduction

in them by 54% and 32%, respectively. This strongly indicates that alumina plateletes are capable of strikingly improving the flame retardancy of PA612 in tems of the reduction in pHRR and THR. On the other hand, the increase in the thermal conductivity of PA612 composites due to the addition of alumina platelets seems to only slightly effect on the flame retardancy effect of 2D alumina on the PA612 composites, namely the thermal conductivity of the composites increases while the PHRR continues to reduce with increasing alumina platelets contents. In addition, when the Al_2O_3 content was above 30 wt%, the thermal conductivity dropped a little while the PHRR continues to decrease. This mainly because the relative content of flammable PA612 reduces while the relative content of non-flammable alumina platelets increases, thus leading to the reduction in the PHRR of the composites. Moreover, the increased residue char can also contribute to reducing the PHRR due to the increase of alumina platelets, as shown in Table 2.

Similar phenonmenon was also observed by Nicolas Cinausero *et al.* in their PMMA and PS nanocomposites filled with alumina nanoparticles. Moreover, they attributed the improved flame retardancy to both physical and physico-chemical processes due to the presence of the nanoscale alumina in the condensed phase [24,25]. With regard to our system we believe that as-observed enhanced flame resistance is most likely due to the physically thermal barrier effect of thermally stable 2D alumina platelets, as evidenced by the monotonous increase in the char residue with increasing alumina content after tests (Fig. 6B and Table 2). Similar reductions in heat release were also observed in the polymer nanocomposites filled with other 2D materials including MoS_2, clay and graphite and its derivatives [18-23].

In terms of the smoke evolved during combustion, it can be expressed by both total smoke production (TRP) and average specific extinction area (ASEA). The PA612

matrix exhibits a TSP of 2.89 m^2/m^2 and ASEA of 342 m^2/kg, suggesting much smoke evolved during burning. By contrast, both smoke parameters gradually decrease with increasing loading level of alumina platelets, strongly demonstrating that the presence of alumina can reduce the smoke production of PA612 during combustion (see Fig. 6D and Table 2). For instance, incorporating 40 wt% of 2D alumina platelets leads TSP and ASEA to reducing down to 2.06 m^2/m^2 and 257 m^2/kg, basically reduced by 29% and by 25%, respectively. Such reduction in the smoke release is extremely meaningful since it can help the trapped people reduce the inhalation of toxic gases and solid particles and largely increase their possibility of survival during fire.

As shown in Table 3, PA612 shows a LOI value of 25.0 %, basically the same as given by the company, indicating it has certain flame retardancy. Upon loaded with alumina platelets, the LOI value rises streadily with increasing alumina content, e.g. a LOI of 27.0 % for PA/10% AP and 29.0 % for PA/30% AP. Such enhancement in LOI values enables PA612 composites to reach a relatively high rating of flame retardancy and to satisfy the flame-retardant requirement in industry. This strongly suggests that the addition of alumina platelets can stengthen the fire safety of PA612. In addition, UL-94 results indicate that the PA612 matrix shows a V-2 rating during vertical burning tests, and bascailly adding less 20 wt% of alumina platelets hardly increases the rating. Once the loading level reaches or above 20 wt%, a V-1 rating can be achieved for all PA612 composites. Moreover, PA612 and all its composites are observed to burn without dripping during UL-94 measurements. Therefore, it is reasonable to conclude that 2D alumina platelets can be one novel potential flame retardant candidate for polymeric materials through the physically thermal barrier role that 2D alumina platelets play in the condensed phase.

3.6. Char residue

Investigating the structure and morphology of char residues after cone tests can help us understand the flame retardancy mechanism since alumina platelets primarily play the role in the condensed phase. As shown in Fig. 8, for the PA612 matrix only a very little char is observed to be in the inner edge of the sample holder. This is mainly because at elevated temperatures small molecules created from the degradation of the underlying polymer diffuse into the flame zone through bubbling, which gradully pushes the char residue to around with combustion. In comparison, with the addition of alumina platelets more char residues are left, and a continuous, intact and thick char layer is achieved as the loading level of alumina increases up to 40%. Moreover, some small holes are also clearly observed on the char surface due to bubbling during burning. This increased char residue layer is primarily responsible for the improved fire retardancy performance of PA612 via the physical barrier effect.

3.7. Rheological behavior

The rheological behaviour of PA612 composites can reflect the melt processing property and also contribute to understanding the flame retardancy mechanism [40-43]. As shown in Fig. 9, the pure PA612 displays a typically viscoelastic behaviour of a linear polymer, namely storage modulus (G) increases whereas complex viscosity (η^*) decreases with increasing frequency. Upon the incorporation of alumin platelets both G and η^* dramtically increase with increasing loading levels in the whole frequency range, which is particularly obvious at the relatively low frequency. For example, adding 20 wt% and 40 wt% of alumina platelets enable the G at 0.01 rad/s to increase from 1.14 Pa (PA612) to 7.51Pa (increase by around 7 times) and 56.7 Pa (increase by 50 times), repectively, showing the reinforcing effect of alumina platelets on PA612. Interestingly, a so-called second plateau is clearly achieved (see Figure 9A)

when the loading level of alumina reaches 40 wt%. Such plateau has been widely regarded as an indication for the formation of a network-like structure, widely observed in many polymer nanocomposites filled with nanoparticles such as clay and carbon nanotubes, once the loading level is above the percolation value of fillers [40-42]. Hence, 40 wt% can be considered as the critical percolation content of as-used 2D alumina platelets, and this much higher threshhold value is mainly due to the relatively lower aspect ratio (~35) of alumian platelets than other anisotropic nanofillers like carbon nanotubes with a typical aspect ratio of over 100 [16]. Most importantly, the 3D physical network of alumina platelets is likely to be responsible for considerable increase in the thermal and flame retardancy properties by acting as a physical barrier.

Likewise, the presence of 40 wt% alumina makes the η^* rise from 400 Pa.s (for PA612) to 4563 Pa.s, an increase by one order of magnitude. High loading levels of 2D alumina platelets can remarkably restrict their free movements by abosorbing many PA612 chains on the surface via strongly hydrogen bond interactions, thus leading to such prominent increase in metl viscosity. It is widely accepted that the fire behaiour is usually governed by the changed melt viscosity of polymer composites [16]. Therefore, the increased viscosity, especially can contribute to slowing down the diffusion speed of oxygen within the polymer melt and the evolution of degradation products from beneath. In addition, the increase of melt viscosity can also help restrict the dripping of the melt during combustion. As a result, the flame resistance can be improved to some extent.

Our previous work has shown a close relationship between peak release rate and storage modulus in the polypropylene nanocomposites [23]. To correlate the viscoelastic behaviour and the flammabily (heat release) for PA612 composites

system, the plots of ralative G' (G'_c/G'_m) and η^* (η^*_c/η^*_m) versus the reciprocal of relative pHRR ($pHRR_m/pHRR_c$) are made (subscripts, c and m, refer to the composite and the polymer matrix, respectively). It is clear from Figure 10 that a good linear relationship between $pHRR_m/pHRR_c$ and G'_c/G'_m or η^*_c/η^*_m is found, as given in Eq.9 and Eq.10 below.

$$G'_c/G'_m = 11\times\frac{pHRR_m}{pHRR_c} - 11 \qquad (9)$$

$$\eta^*_c/\eta^*_m = 3.5\times\frac{pHRR_m}{pHRR_c} - 2.8 \qquad (10)$$

However, one deviation is also observed for PA612/40% AP, probably due to the formation of a physical network of alumina platelets, thus leading to a drastic change in the properties. Despite that, it is still reasonable to conlude that increased storage modulus and melt viscosity, especially the formation of 3D physical network, can contribute to the largely enhanced flame retardancy of PA612.

4. Conclusions

High-performance PA612 composites filled with 2D alumina platelets have been successfully fabricated via melt blending in this work. Alumina platelets are found be homogeneously dispersed in the polymer matrix due to the strong interfacial hydrogen bond interactions. The presence of alumina platelets is able to significantly increase thermal stability (T_i and T_{max}) of PA612 because of the physical barrier effect. Meanwhile, the thermal conductivity (λ) increases by 44% (up to 0.46 W/mK) upon the addition of 20 wt% alumina. In addition, adding alumina platelets can noticeably improve the flame retardancy of PA612 in terms of the marked reduction in the heat release rate and smoke production mainly due to the physcial barrier effect of 2D alumina on both oxygen and small molecular degrdation products or fuels. Most

importantly, we have successfully established a basically qualitative relationship between the flammability (peak heat release rate) and viscoelastic behaviour (G and η^*). This work offers a new approach for creating advanced thermally stable, conductive and flame-retardant polymer composites by using 2D alumina platelets as functional filler.

Author Contributions

[#]Cong Sun, Lei Chen and Yiqi Sun contribute equally to this work as co-first author.

Notes

The authors declare no competing financial interest.

Acknowledgements

This work was supported by the Scientific Research Foundation of Zhejiang A&F University (Grant No. 2055210012); the National Natural Science Foundation of China (Grant No. 51303162, 21404092, 51505432 and 51628302); the Zhejiang Provincial Natural Science Foundation of China (Grant No. Q15C160002); the Commonwealth Project of Science and Technology Agency of Zhejiang Province of China (Grant No. 2017C37078); the Program for Key Science and Technology Team of Zhejiang Province (Grant No. 2013TD17); and the Science and Technology Project of Taizhou City (Grant No. 14GY01).

References

[1] Li HZ, Wu YJ, Sato H, Kong L, Zhang CF, Huang K., et al. A new facile method for preparation of nylon-6 with high crystallinity and special morphology. Macromolecules 2009; 42(42): 1175-1179.

[2] Huang M, Feng J, Wang J, Zhang X, Li Y, Yan Y. Synthesis and characterization of nano-HA/PA66 composites. J Mater Sci Mater Med 2003; 14(7): 655-660.

[3] Martino L, Basilissi L, Farina H, Ortenzi MA, Zini E, Silvestro GD, Scandola M. Bio-based polyamide 11: Synthesis, rheology and solid-state properties of star structures. Eur Polym J 2014; 59: 69-77.

[4] Kumar S, Maiti SN, Satapathy BK. Super-toughening polyamide-612 by controlling dispersed phase domain size: Essential work of fracture assessment. Mater Des 2014; 62(10): 382-391.

[5] Kumar S, Satapathy SN, Maiti BK. Correlation of morphological parameters and mechanical performance of polyamide-612/poly (ethylene-octene) elastomer blends. Polym Adv Technol 2013; 24(5): 511-519.

[6] Wang LL, Dong X, Gao YY, Huang MM, Han CC, Zhu SN, Wang DJ. Transamidation determination and mechanism of long chain-based aliphatic polyamide alloys with excellent interface miscibility. Polymer 2015; 59: 16-25.

[7] Chen YH, Wang Q, Yan W, Tang H.M. Preparation of flame retardant polyamide 6 composite with melamine cyanurate nanoparticles in situ formed in extrusion process. Polym Degrad Stab 2001; 91(11): 2632-2642.

[8] Fei GX, Liu Y, Wang Q. Synergistic effects of novolac-based char former with magnesium hydroxide in flame retardant polyamide-6. Polym Degrad Stab 2008 93(7): 1351-1356.

[9] Sergei VL, Edward DW. Combustion and fire retardancy of aliphatic nylons. Polym Int 2000; 49(10): 1033-1073.

[10] Balabanovich A I, Levchik GF, Levchik SV, Schnabel W. Fire retardance in polyamide-6. The effects of red phosphorus and radiation-induced cross-links, Macromol Mater Eng 2001; 25(5): 179-184.

[11] Liu Y, Wang Q. Melamine cyanurate-microencapsulated red phosphorus flame retardant unreinforced and glass fiber reinforced polyamide 66. Polym Degrad Stab 2006; 91(12): 3103-3109.

[12] Siat C, Bourbigot S, Le BM. Thermal behaviour of polyamide-6-based intumescent formulations-a kinetic study. Polym Degrad Stab 1997; 58(3): 303-313.

[13] Le BM, Bourbigot S, Felix E, Pouille F, Siat C, Traisnel M, Le BM, Bourbigot S., Felix E, Pouille F, Siat C, Traisnel M. Characterization of a polyamide-6-based intumescent additive for thermoplastic formulations. Polymer 2000; 41(14): 5283-5296.

[14] Chen YH, Wang Q. Preparation, properties and characterizations of halogen-free nitrogen-phosphorous flame-retarded glass fiber reinforced polyamide 6 composite. Polym Degrad Stab 2006; 91(9): 2003-2013.

[15] Rothon RN, Hornsby PR. Flame retardant effects of magnesium hydroxide. Polym Degrad Stab. 1996; 54(2-3): 383-385.

[16] Schartel B, P tschke P, Knoll U, Abdel-Goad M. Fire behaviour of polyamide 6/multiwall carbon nanotube nanocomposites. Eur Polym J 2005; 41(5):1061-1070.

[17] Mancic L, Osman RFM, Costa AMLM, d'Almeida JRM, Marinkovic BA, Rizzo FC. Thermal and mechanical properties of polyamide 11 based composites reinforced with surface modified titanate nanotubes. Mater Des 2015; 83: 459-467.

[18] Kashiwagi T, Harrris Jr RH, Zhang X, Briber RM, Cipriano BH, Raghavan SR, Award WH, Shields JR. Flame retardant mechanism of polyamide 6–clay nanocomposites. Polymer 2004; 45(3): 881-891.

[19] Jiang SD, Tang G, Bai ZM, Wang YY, Hu Y, Song L. Surface functionalization of MoS_2 with POSS for enhancing thermal, flame-retardant and mechanical properties in PVA composites. RSC Adv 2014; 4(7): 3253-3262.

[20] Zhou KQ, Tang G, Jiang SH, Zhou G, Hu Y. Combination effect of MoS_2 with aluminum hypophosphite in flame retardant ethylene-vinyl acetate composites. RSC Adv 2016; 6(44): 37672-37680.

[21] Jin YX, Huang GB, Han DM, Song PA, Tang WY, Bao JS, Li RR, Liu YL. Functionalizing graphene decorated with phosphorus-nitrogen containing dendrimer for high-performance polymer nanocomposites. Comp Part A 2016; 86: 9-18.

[22] Huang GB, Song PA, Liu LN, Bao JS, Ge CH, Li RR, Guo QP. Fabrication of multifunctional graphene decorated with bromine and nano-Sb_2O_3 towards high-performance polymer nanocomposites. Carbon 2016; 98: 689-701.

[23] Song PA, Yu YM, Zhang T, Fu SY, Fang ZP, Wu Q. Permeability, viscoelasticity, flammability performances and their relationship of polymer nanocomposites. Ind Eng Chem Res 2012; 51(21): 7255-7263.

[24] Cinausero N, Azema N, Lopez Cuesta JM, Cochez M. Ferriol Impact of modified alumina oxides on the fire properties of PMMA and PS nanocomposites. Polym Adv Technol 2011; 22(12): 1931-1939.

[25] Cinausero N, Azema N, Cochez M, Ferriol M, Essahli M, Ganacharud F, Lopez Cuesta JM. Influence of the surface modification of alumina nanoparticles on the thermal stability and fire reaction of PMMA composites. Polym Adv Technol 2008; 19(6): 701-709.

[26] Bonderer LJ, Studart AR, Gauckler LJ. Bioinspired design and assembly of platelets reinforced polymer films. Science 2008; 319: 1069-1073.

[27] Qian MB, Sun YQ, Xu XD, Liu LN, Song PA, Yu YM, Wang H, Qian J. 2D-alumina platelets enhance mechanical and abrasion properties of PA612 via interfacial hydrogen-bond interactions. Chem Eng J 2017; 308: 760-711.

[28] Goodman I, Kehayoglou AH. Anionic copolymers of caprolactam with laurolactam (nylon 612 copolymers). II. Crystallisation, glass transitions and tensile properties. Eur Polym J 1983; 19(4): 321-325.

[29] Rusu G, Rusu E. Evaluation of thermal and dielectric behaviour of some anionic nylon 612 copolymers. Mater Des 2010; 31(10): 4601-4610.

[30] BudÍn J, Brožek J, Roda J. Polymerization of lactams, 96 anionic copolymerization of -caprolactam with ω-laurolactam. Polymer 2006; 47(1): 140-147.

[31] Song PA, Xu ZG, Guo QP. Bioinspired strategy for tuning thermal stability of PVA via hydrogen-bond crosslink. Comp Sci Technol 2015; 118: 16-22.

[32] Song PA, Xu ZG, Guo QP. Bioinspired srategy to reinforce PVA with improved toughness and thermal properties via hydrogen-bond self-assembly. ACS Macro Lett 2013; 2(12): 1100-1104.

[33] Fu JF, Shi LY, Zhong QD, Chen Y, Chen LY. Thermally conductive and electrically insulative nanocomposites based on hyperbranched epoxy and nano-Al_2O_3 particles modified epoxy resin. Polym Adv Technol 2010; 22(6): 1032-1041.

[34] Zhang S, Cao XY, Ma YM, Ke YC, Zhang JK, Wang FS. The effects of particle size and content on the thermal conductivity and mechanical properties of Al_2O_3/high-density polyethylene (HDPE) composites. Express Polym Lett 2011; 5(7): 581-590.

[35] Mamumnya Ye P, Davydenko VV, Pissis P, Lebedev EV. Electrical and thermal conductivity of polymers filled with metal powders. Eur Polym J 2002; 38(9): 1887-1897.

[36] Salazar A, Sanchez-Lavenga A, Terron JM. Effective thermal diffusivity of layered materials measured by modulated photothermal techniques. J Appl Phys 1998; 84(84): 3031-3041.

[37] Liu LN, Huang GB, Song PA, Yu YM, Fu SY. Converting industrial alkali lignin to biobased functional additives for improving fire behavior and smoke suppression of polybutylene succinate. ACS Sustainable Chem Eng 2016; 4: 4732-4742.

[38] Liu LN, Qian MB, Song PA, Huang GB, Yu YM, Fu SY. Fabrication of green lignin-based flame retardants for enhancing the thermal and fire retardancy properties of polypropylene/wood composites. ACS Sustainable Chem Eng 2016; 4: 2422-2431.

[39] Song PA, Zhao LP, Cao ZH, Fang ZP. Polypropylene nanocomposites based on C60-decorated carbon nanotubes: thermal properties, flammability, and mechanical properties. J Mater Chem 2011; 21(21): 7782-7788.

[40] Kashiwagi T, Du FM, Winey KI, Cipriano B, Rahavan SR, Pack S, Rafailovich M, Yang Y, Grulke E, Shields J, Harris RH, Douglas JF. Relation between the viscoelastic and flammability properties of polymer nanocomposites. Polymer, 2008; 49(20) 4358-4368.

[41] Kashiwagi T, Du FM, Douglas JF, Winey KI, Harris RH, Shields JJR. Nanoparticle network reduce the flammability of polymer nanocomposites. Nat Mater 2005; 4(12): 928-933.

[42] Song PA, Xu LH, Guo ZH, Zhang Y, Fang ZP. Flame retardant wrapped carbon nanotubes for simultaneously improving the flame retardancy and mechanical properties of polypropylene. J Mater Chem 2008; 18(42): 5083-5091.

Figure Captions

Fig. 1. A) SEM image and B) TEM image of as-used alumina platelets (AP) and SEM images showing the dispersion of AP in PA612 matrix: C) PA/5% AP, D) PA/10% AP, E) PA/20% AP, and F) PA/40% AP.

Fig. 2. DSC thermograms of a) PA612, b) PA/5% AP, c) PA/10% AP, d) PA/20% AP, e) PA/30% AP and f) PA/10% AP at a heating rate of 10 ^{o}C/min.

Fig. 3. A) TGA and B) DTG curves of PA612 and its composites in nitrogen condition. ^{a} T_i and T_{max} refer to the thermal degradation temprature where 5 wt% mass loss occurs and the temperature where the maximum weight loss takes place, respectively.

Fig. 4. A) TGA and B) DTG curves of PA612 and its composites in air condition. ^{a} T_i and T_{max} refer to the thermal degradation temprature where 5 wt% mass loss occurs and the temperature where the maximum weight loss takes place, respectively.

Fig. 5. Correaltion between two typical thermal stability parameters (T_i and T_{max}) and volume fractions of alumina platelets of PA612 and its composites: A) in nitrogen and B) in air atmosphere.

Fig. 6. Thermal conductivity of PA612/AP composites as a function of the volume fraction of AP together with theoretical prediction values by Eqs. 6-8.

Fig. 7. Flammability performances of PA612/AP composites evaluated by cone tests: A) heat release rate, B) normalized mass loss, C) total heat release, and D) total smoke production at an incident heat flux of 35 kW/m^2.

Fig. 8. Morphology of char residue for A) PA612 bulk, D) PA/10% AP,E) PA/20% AP, and F) PA/40% AP collected after cone measurements.

Fig. 9. Frequecy (ω) dependence of A) storage modulus (G□) and B) complex viscosity (η^*) for PA612 and its composites at 220 °C.

Fig. 10. Correlation between peak of heat release and viscoelastic properties of PA612 and its composites.

Figure 1

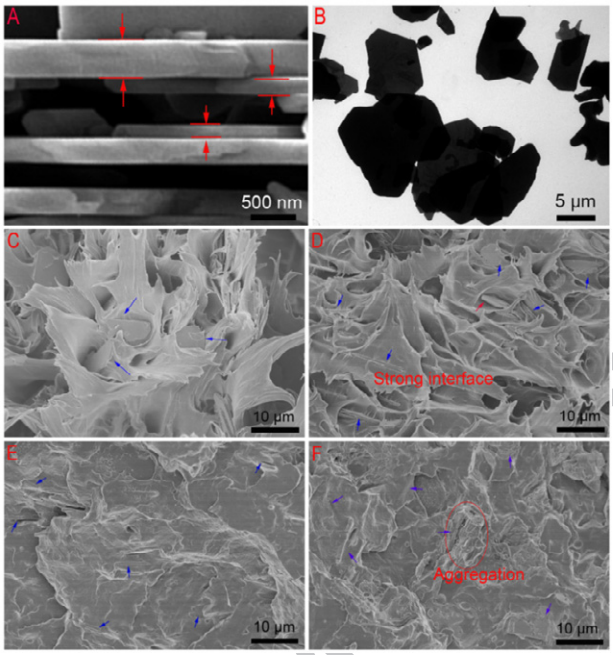

Figure 2

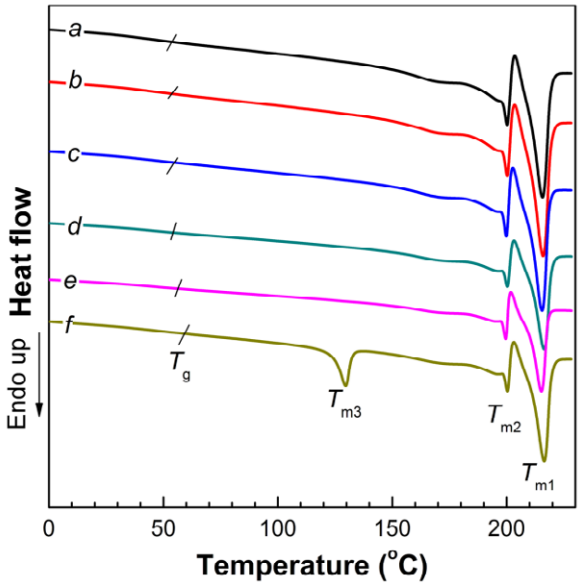

Figure 3

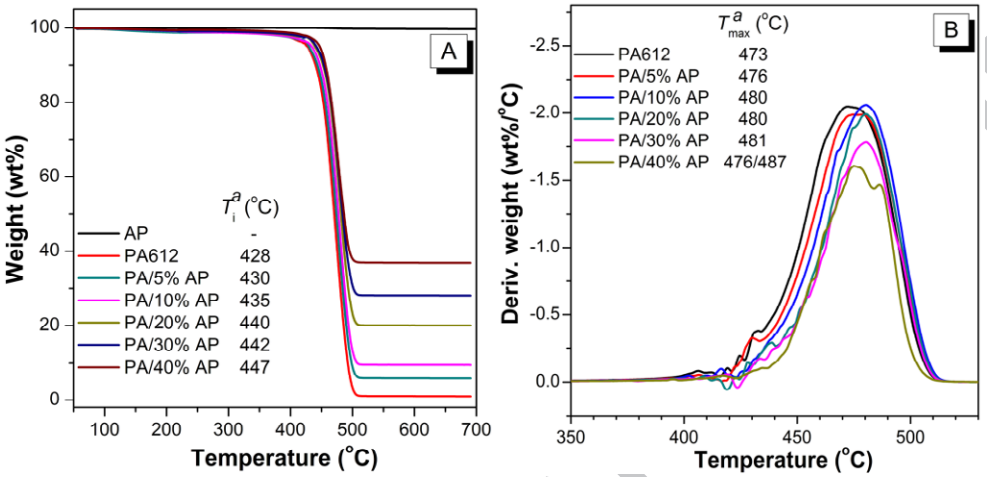

Figure 4

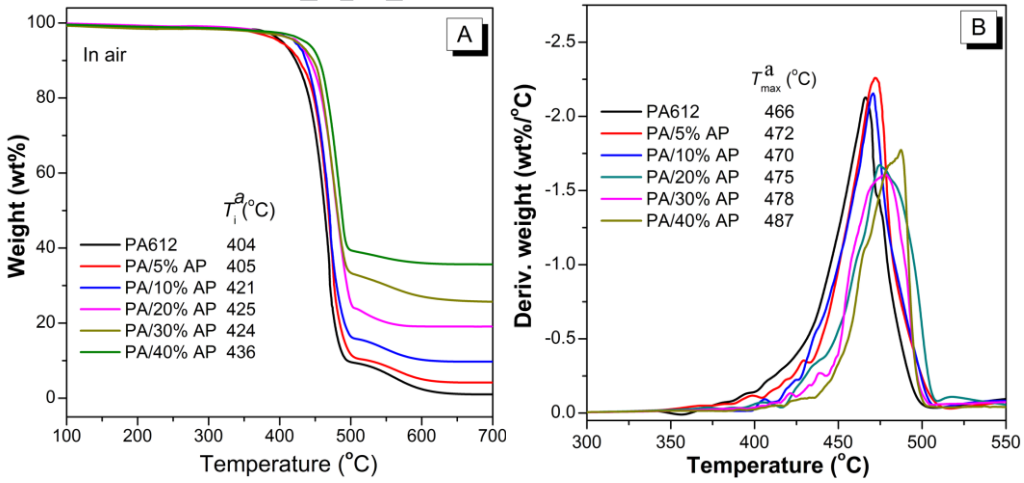

Figure 5

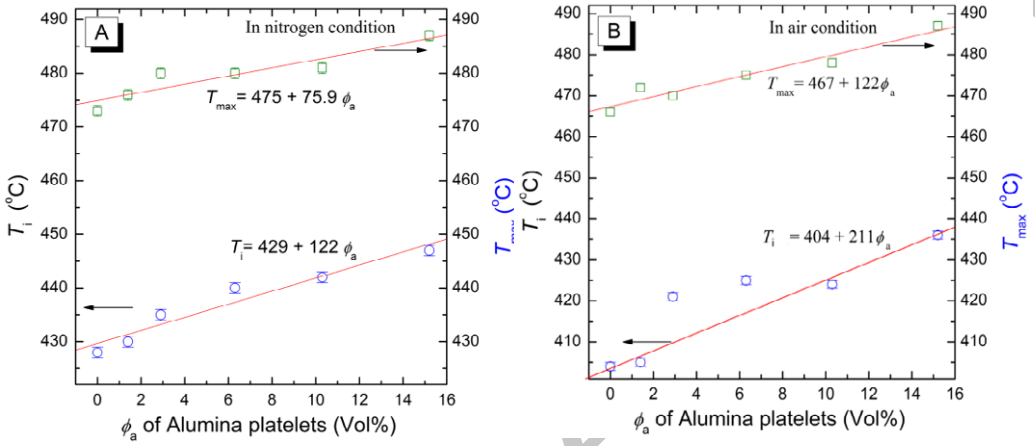

Figure 6

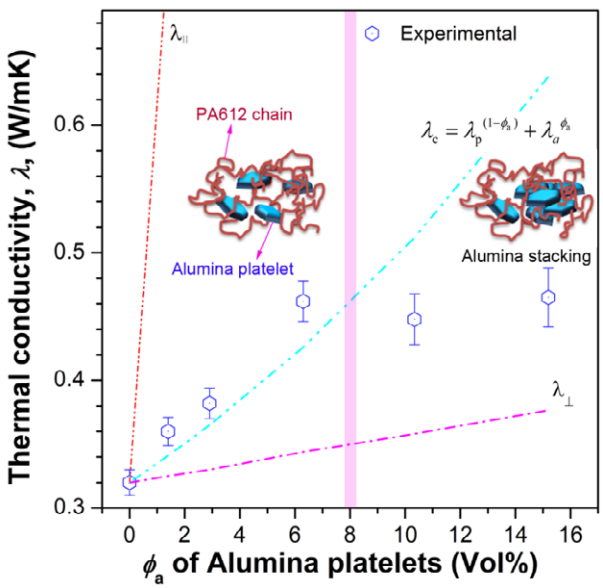

Figure 7

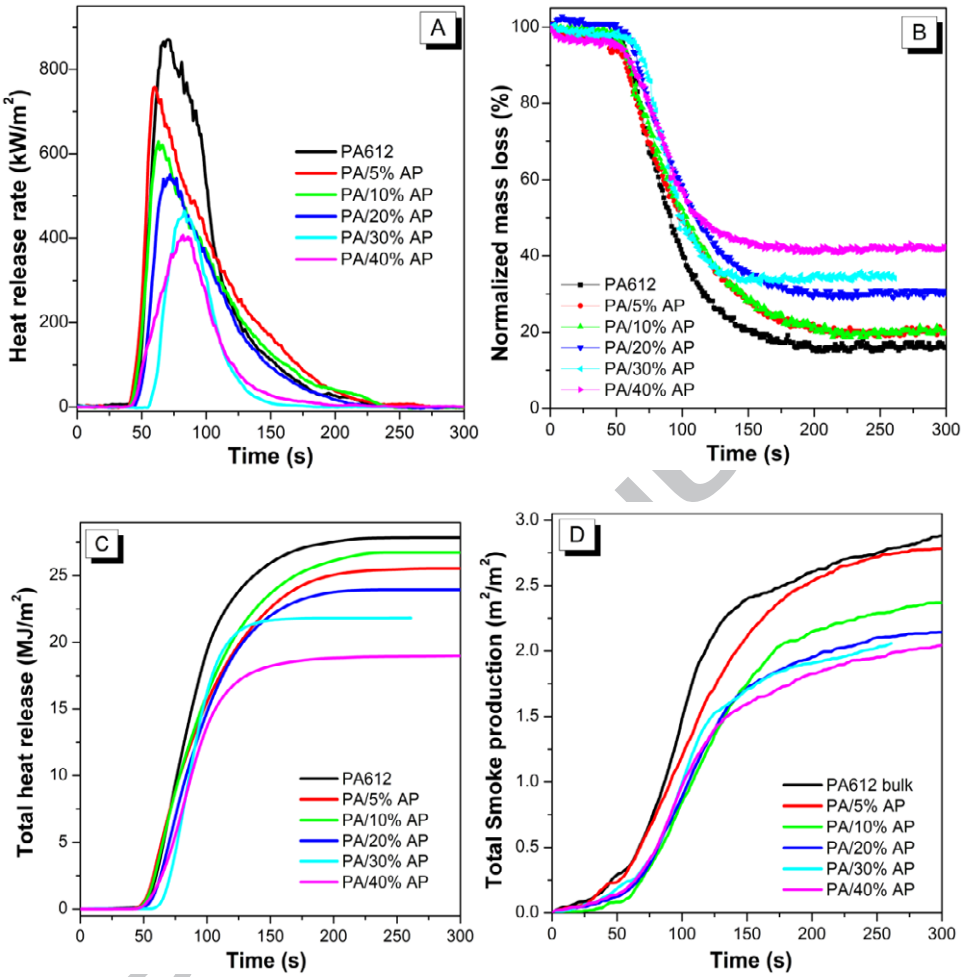

Figure 8

Figure 9

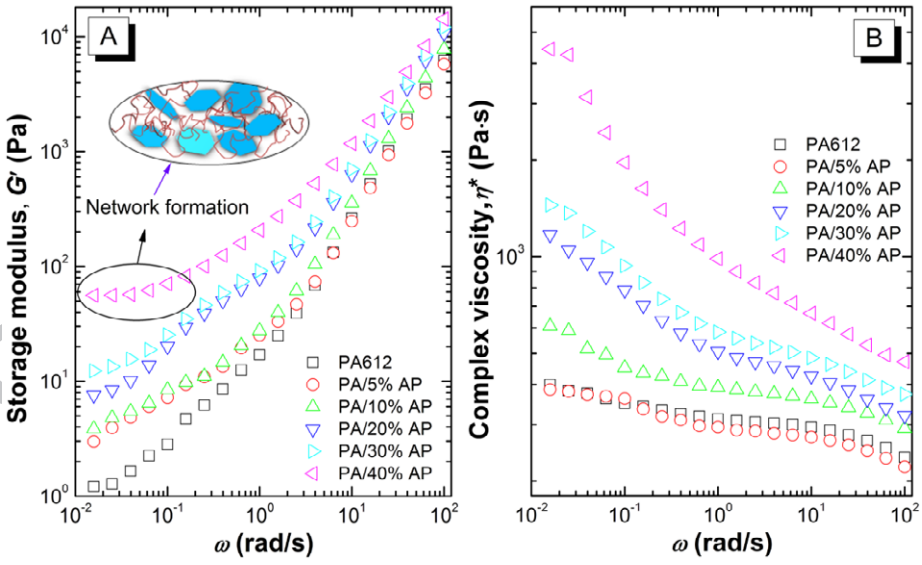

Figure 10

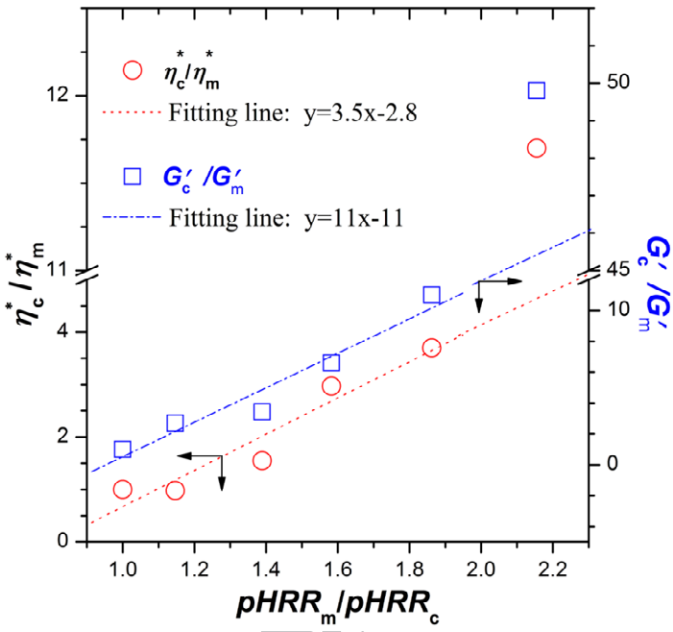

Table 1 Detailed thermal property parameters of PA612 and its composites filled with alumina platelets collected from DSC measurements.

Run	T_g [a] (°C)	T_m [a] (°C)			ΔH_m [a] (J/g)			χ_c [a]
		T_{m1}	T_{m2}	T_{m3}	ΔH_{m1}	ΔH_{m2}	ΔH_{m3}	(%)
PA612 bulk	56.8	215.6	200.3		34.1	13.5		18.4
PA/5% AP	57.3	215.8	200.4		33.8	13.1		18.2
PA/10% AP	58.6	215.3	200.0		36.7	13.3		18.4
PA/20% AP	57.9	216.2	200.4		35.9	12.4		18.3
PA/30% AP	58.6	215.1	199.6		35.3	12.3		18.5
PA/40% AP	60.2	216.3	200.3	129.6	22.0	6.66	6.05	13.5

[a] T_g, T_m, ΔH_m and χ_c refer to the glass transition temperature, melting point, heat of fusion, and degree of crystallinity, respectively.

Table 2 Detailed parameters obtained from cone measurements for PA612 and its composites filled with alumina platelets.

Run	t_{ign} [a] (s)	pHRR [a] (kW/m^2)	THR [a] (MJ/m^2)	TSP [a] (m^2/m^2)	ASEA [a] (m^2/kg)	char [a] (wt%)
PA612	46±1	875±50	27.9±0.8	2.89±0.3	342±18	16.1±0.3
PA/5% AP	42±1	763±42	25.6±0.7	2.78±0.3	333±15	20.2±0.3
PA/10% AP	42±1	630±40	26.3±0.7	2.36±0.2	309±16	21.5±0.4
PA/20% AP	45±1	553±35	23.9±0.5	2.14±0.2	302±15	30.5±0.5
PA/30% AP	57±1	470±28	21.7±0.5	2.06±0.2	290±13	34.6±0.5
PA/40% AP	44±1	406±25	19.0±0.4	2.04±0.3	257±10	41.9±0.6

[a] t_{ign}, pHRR, THR, TSP, ASEA and char refer to the time to ignition, peak heat release rate, total heat release, total smoke production, and char residues after cone test, respectively.

Table 3 Detailed data collected from LOI and UL-94 tests for PA612 and its composites filled with alumina platelets.

Run	LOI [a] (vol.%)	Dripping Y/N	UL-94 rating
PA612	25.0	N	V-2
PA/5% AP	25.5	N	V-2
PA/10% AP	27.0	N	V-2
PA/20% AP	28.0	N	V-1
PA/30% AP	29.0	N	V-1
PA/40% AP	29.5	N	V-1

Graphic Abstract